Available online at www.sciencedirect.com
ScienceDirect
Journal of Hazardous Materials 155 (2008) 65–75
Journal of Hazardous Materials
www.elsevier.com/locate/jhazmat

Adsorption of Cr(VI) from aqueous solutions by spent activated clay

Chih-Huang Weng [a,*], Y.C. Sharma [b], Sue-Hua Chu [a]

[a] *Department of Civil and Ecological Engineering, I-Shou University, Da-Hsu Township, Kaohsiung 84008, Taiwan*
[b] *Environmental Engineering and Research Laboratories, Department of Applied Chemistry, Institute of Technology, Banaras Hindu University, Varanasi 221005, India*

Received 11 July 2007; received in revised form 20 October 2007; accepted 11 November 2007
Available online 17 November 2007

Abstract

Adsorption of Cr(VI) onto spent activated clay (SAC), a waste produced from an edible oil refinery company, was investigated for its beneficial use in wastewater treatment. After pressure steam treatment, SAC was used as an adsorbent. The adsorption kinetic data were analyzed and fitted well in a pseudo-first-order equation and the rate of removal was found to speed up with decreasing pH and increasing temperature. Activation energy for the adsorption process was found to be 4.01–5.47 kcal/K mol. The Langmuir adsorption isotherm was used to fit the equilibrium data and the effect of pH, temperature and ionic strength were studied. The maximum adsorption capacities for Cr(VI) ranged from 0.743 to 1.422 mg/g for temperature between 4 and 40 °C under a condition of pH 2.0. The studies conducted show the process of Cr(VI) removal to be spontaneous at high temperature and endothermic in nature. From the waste utilization and environment point of view, the work carried out is important and useful. Results obtained can serve as baseline data for designing a treatment process using this low-cost adsorbent for the treatment of wastewater rich in Cr(VI).

Keywords: Activated clay; Adsorption; Chromium; Equilibrium; Kinetics

1. Introduction

Trivalent chromium (Cr(III)) and hexavalent chromium (Cr(VI)) are the two common existing oxidation states of chromium found in the environment. Public concerns over Cr are mostly related to Cr(VI) due to its high toxic nature to biological systems. Major sources of chromium to aquatic systems are effluents from electroplating, metal finishing, magnetic tapes, pigments, leather tanning, wood protection, chromium mining and milling, brass, electrical and electronics' equipments manufactures and catalysis [1]. Improper treatment of the Cr effluents will pose a serious problem to ecosystems and causes great public concern. U.S.EPA [2] has fixed an enforceable maximum contamination level for Cr in drinking water of 0.1 mg/L for public water system. Removal of Cr from these effluents is deemed necessary not only for the protection of aquatic environments but also a requirement for compliance with the stringent discharge limits.

Amongst the viable technologies developed for removal of Cr(VI) from industrial wastewater, conventionally, chemical reduction followed by precipitation is the most common method used for compliance with regulation limits. The drawbacks of using this approach are the consumption of chemical agents and the generation of large amount of sludge. Other methods, such as ion exchange, reverse osmosis, electrodialysis and membrane separation may be used for Cr(VI) decontamination. However, they are not economically viable because the operational cost is relatively high. Adsorption offers an alternative technology for removal of heavy metals and dyes from wastewater. With the selection of a proper adsorbent, the adsorption process can be a promising and effective technique for the removal of certain types of contaminants [3]. Activated carbon has broadly been applied for wastewater treatment as one of the most effective adsorbents to remove a variety of contaminants. The activated carbon, upon reaching its adsorption capacity, is either disposed to landfill or regenerated at elevated temperature. The use of activated carbon has the following disadvantages: high adsorbent cost, loss of adsorption capacity after regeneration and difficulties of operation. Thus, many researchers have focused on seeking the low-cost adsorbents as alternates to activated carbon.

* Corresponding author. Tel.: +886 7 6578957; fax: +886 7 6577461.
E-mail address: chweng@isu.edu.tw (C.-H. Weng).

0304-3894/$ – see front matter © 2007 Elsevier B.V. All rights reserved.
doi:10.1016/j.jhazmat.2007.11.029

In particular, one thorough review paper [4] and recent studies [5–7] have looked into the low-cost adsorbents for removal of heavy metals. To keep this issue on track, most recently, Mohan and Pittman Jr. [1] have published one fruitful review paper on chromium removal by adsorption. Basically, the broad low-cost adsorbents can be divided into three categories: (1) biomass, (2) agriculture and industrial wastes and (3) nano-sized particles. Despite the fact that low-cost adsorbents have been intensively studied for many years, study of the use of spent activated clay (SAC), an industrial waste, in treating wastewater enriched with Cr(VI) has not yet been found in literature and the authors claim to be frontrunners in using SAC for removal of chromium.

The present paper reports the results for kinetic and equilibrium studies of Cr(VI) adsorption onto SAC. Since the effectiveness of adsorption relies much on operational conditions, parameters that may affect the adsorption including pH, temperature and ionic strength were evaluated. Both kinetic and equilibrium isotherm models were applied to establish the rate of adsorption, adsorption capacity and the mechanism of Cr(VI) adsorption onto SAC. Results of this study will be useful for future scale up and can also serve as base-line data for using this waste as a low-cost adsorbent for treatment Cr(VI)-rich effluents.

2. Materials and methods

2.1. Spent activated clay

The raw spent activated clay (RSAC) was obtained from an edible oil refinery company in southern Taiwan. While the annual production of RSAC in this company alone is about 2500–3000 tonnes, utilization of this waste has not yet taken place. The commercial virgin activated clay provided to the edible oil company is originated from montmorillonite which was chemically activated by sulfuric acid. After the clay was used to remove color from oil, the color of the activated clay would change from white to brown. To recover more activated sites for adsorption, the RSAC sample was treated as follows: (1) mix 250 g RSAC sample with 2 L distilled water; (2) place the solution in a high pressure cooker (S-328, First Lady, Taiwan) under a pressure of 10 psi at 100 °C for 15 min cooking; (3) remove the supernatant and rinse the cooked sample with distilled water; (4) run the process from step (1) to (3) for a number of times until the supernatant is free of water and turbidity; (5) dry in an oven overnight and store in a desiccator for use as adsorbent. The particle size of treated spent activated clay (SAC) of less than 74 μm was used in the experiments.

The morphological characteristics of SAC were evaluated using a scanning electron microscope (SEM) equipped with energy dispersive X-ray spectroscopy (EDS) (Hitachi S2700). Samples of SAC were all gold plated and an electron acceleration voltage of 20 kV was applied for SEM observation. Fig. 1 shows the SEM micrographs of the SAC sample at 5000 times magnification. It can be seen from Fig. 1a, that the blurred image showing the surface of raw SAC particles was covered by oily-like materials and it is almost non-porous. After pressure cooker treatment, the image (Fig. 1b) shows the SAC particle is mostly irregular in shape and has a porous surface. Since SAC is chemically activated montmorillonite (an expanding 2:1 layer silicate mineral), it is expected that the main components of this SAC are SiO_2 and Al_2O_3 [8]. Results of EDS analysis of the adsorbent indicated that its main constituents are O, Si, Al and Fe and Mg are in traces. The appearance of Fe (or Mg) in SAC may result from the substitution for Al^{3+} in the octahedral sheet of the clay mineral. Table 1 outlines some basic properties of SAC. The treated SAC has a pH of 3.12 and was obtained by immersing it in a solution containing 1:1 (v/v) ratio of SAC and distilled water. The low pH value was attributed to the activation procedure by an acid in the manufacturing process. Thus, it can be considered as an acidic adsorbent prevailing for Cr(VI) adsorption at low pH. The specific surface area and average pore radius for the treated

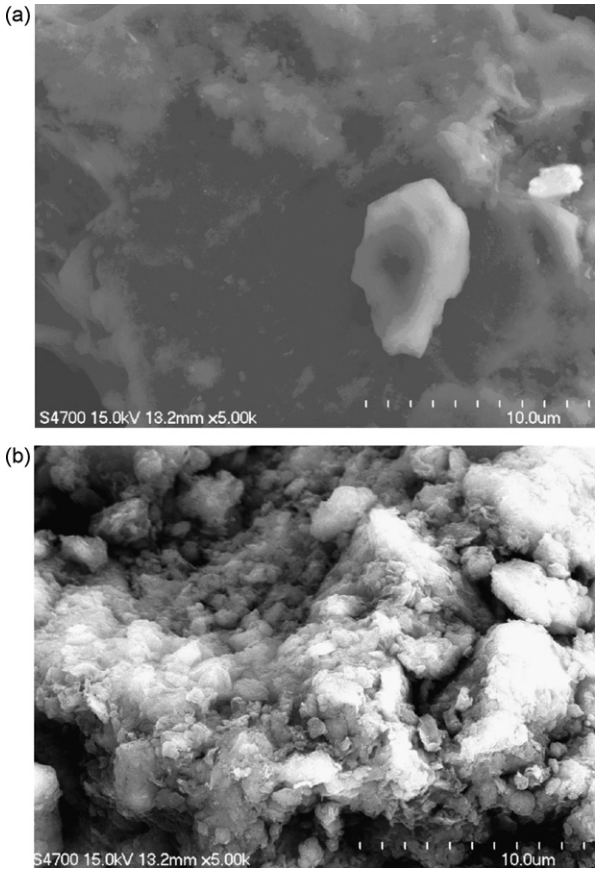

Fig. 1. SEM images of SAC. (a) Before and (b) after treatment by pressure cooker (5000×).

Table 1
Some basic properties of SAC

Parameters	Original SAC	Treated SAC
Average size (μm)	<74.00	<74.00
pH in distilled water	2.76	3.12
pH_{zpc}	3.2	3.8
Oil content (%)	13.15	2.91
BET-N_2 SSA (m^2/g)	1.85	7.42
Pore size (nm)	4.92	6.84

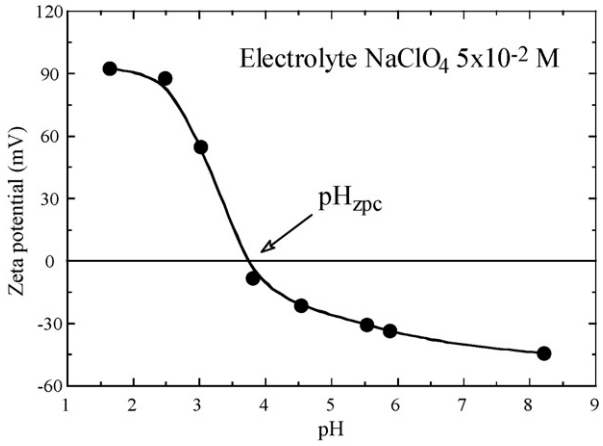

Fig. 2. Zeta potential measurements as a function of pH for SAC.

SAC were measured and found to be 7.42 m^2/g and 6.84 nm, respectively, using a Brunauer, Emmett, Teller (BET) N_2 area analyzer (Coulter SA3100, Beckman). The pH-dependence of the zeta potential of hydrolyzed SAC was determined instrumentally (Laser Zee 3.0, Pen Kem Inc.). A zero point of charge (pH_{zpc}) of the SAC particulates was around 3.8 determined as shown in Fig. 2. The oil content of the treated SAC was found to be 2.91% measured by oil Soxhlet extraction method [9]. It appears that the pretreatment process has rendered SAC with less oil content, thereby increasing pore size and surface area allowable for adsorption.

2.2. Batch adsorption studies

All chemicals used were of AR grade (Pfaltz and Bauer, Stamford, CT, USA). Chromium solution was prepared by dissolving a known quantity of potassium dichromate ($K_2Cr_2O_7$) in double-distilled water. Cr(VI) in the solution was analyzed by reaction with diphenylcarbohydrazide, and subsequently measuring the absorbance of the purple product at a wavelength of 540 nm with a spectrophotometer (Hach DR2010, USA). All the experiments were carried out at a temperature of 24 °C, pH 2.0, and ionic strength of 5×10^{-2} M except as stated otherwise. Standard base of 0.1 M NaOH and acid of 0.1 M HCl solutions were used for pH adjustment. Temperature was controlled by keeping the mixtures in a water circulation bath whose temperature varied within ±0.2 °C. To maintain a constant thermal state, the polyethylene (PE) bottle was first placed into the temperature controlled bath for about 0.5 h prior to the start of the experiments. For the effect of pH on adsorption, the pH of the solution was maintained at 2.0, 2.5, 3.0, 3.5 and 4.0. For the effect of temperature on adsorption, experiments were conducted under isothermal conditions at 4, 14, 24 and 40 °C. Blank tests without adsorbent (SAC) in the mixed suspension were also performed to avoid possible adsorption on the PE bottles and the filter apparatus was used for separation of the adsorbent from the solution. All experiments were replicated and the average values were taken in the data analysis.

Kinetic adsorption experiments were carried out to establish the effect of time on the adsorption process and to determine the rate of adsorption for Cr(VI) removal as affected by pH and temperature. The general experimental procedures are described as follows: (1) prepare 1 L solution containing a certain amount of Cr (6.75 mg/L) with a constant strength of $NaClO_4$ (5×10^{-2} M) in a PE bottle; (2) agitate these solutions on a magnetic stirrer at 300 rpm; (3) adjust solution pH to a desired value; (4) add a given amount of the SAC (1 g/L) into the solution; (5) at the completion of preset time intervals, a 5 mL of solution was taken and immediately filtered via 0.45 μm fiber glass membrane filter (47 mm, Advantec GS25, Japan) to collect the supernatant; (6) determine the residual Cr(VI) concentration in each of the supernatants. The amount of Cr(VI) adsorbed in mg/g at contact time t was calculated as follows:

$$q_t = \frac{C_o - C_t}{w} \quad (1)$$

where C_o (mg/L) and C_t (mg/L) are the initial Cr(VI) concentration and the Cr(VI) concentration at time t, respectively, and w (g/L) is the SAC amount in the solution.

Equilibrium experiments were performed to establish the adsorption isotherms affected by pH, temperature and ionic strength. The isotherm studies were conducted by varying the initial Cr(VI) concentration at room temperature while the adsorbent was kept at 1 g/L. Detailed experimental procedures were described as follows: (1) prepare one 2.0 L solution with a constant ionic strength of 5×10^{-2} M $NaClO_4$ and different Cr(VI) concentrations (0.2–10 mg/L); (2) distribute 100 mL of solution to a series of 125 mL polyethylene (PE) bottles; (3) adjust initial pH to 2.0; (3) add a given amount of the SAC (1 g/L) into the solution; (4) shake these bottles on a reciprocal shaker at 150 excursions/min for 2 h. This contact time was found to be adequate for reaching equilibrium adsorption based on the results of the kinetic study; (5) at the end of shaking, record the final pH of the mixed liquor; (6) separate the adsorbent via the filter paper and the supernatant was collected for Cr(VI) concentration measurement.

3. Results and discussion

3.1. Kinetic studies

A pseudo-first-order (PFO) equation based on the adsorption capacity was used to analyze the adsorption kinetics data. The form of PFO is described as follows [10]:

$$\frac{dq}{dt} = k(q_e - q) \quad (2)$$

where q_e is the amount of Cr(VI) adsorbed at equilibrium (mol/g) and k is the PFO rate constant (min^{-1}). If the initial adsorbed concentration at $t = 0$ has $q_t = 0$ and if at $t = t$, the adsorbed concentration is $q_t = q_t$, then Eq. (2) becomes

$$q_t = q_e \left(1 - \frac{1}{10}^{(k_1/2.303)t}\right) \quad (3)$$

A graphical computer software, viz. KaleidaGraph™ [11], was used for non-linear fitting of the experimental data. The validity of the PFO in describing the kinetic data is checked by the

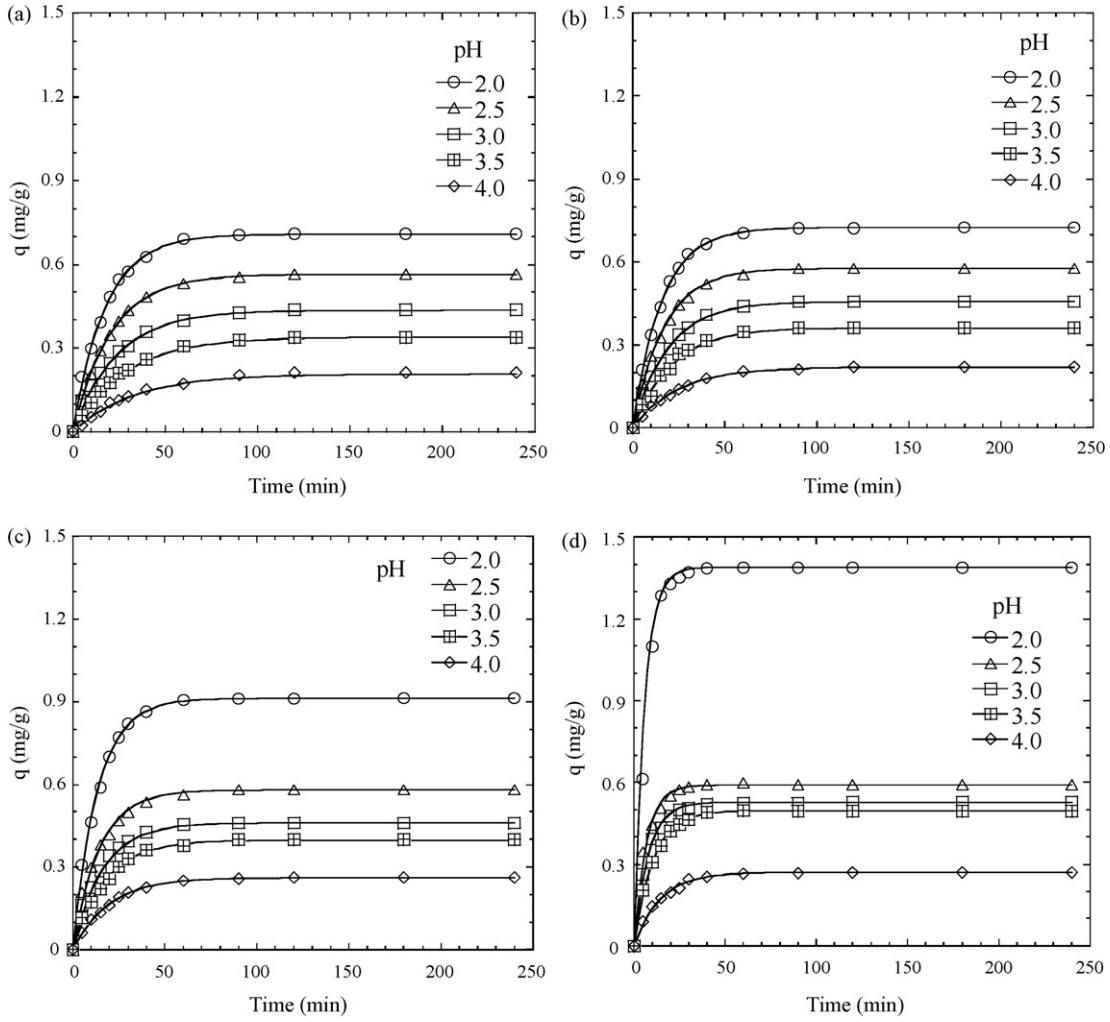

Fig. 3. Time variation of Cr(VI) adsorption onto SAC at different pHs and temperatures. (a) 4 °C; (b) 14 °C; (c) 24 °C; (d) 40 °C. Solid lines are the best fit of pseudo-first-order equation.

least-squares correlation coefficient (r^2) and normalized standard deviation s (%). The s is defined as:

$$s = 100 \times \sqrt{\frac{\sum [(q_{t,\mathrm{exp}} - q_{t,\mathrm{cal}})/q_{t,\mathrm{exp}}]^2}{n-1}} \quad (4)$$

where $q_{t,\mathrm{exp}}$ and $q_{t,\mathrm{cal}}$ are the measured and calculated Cr(V) adsorbed at time t, respectively, and n is the number of data points.

Fig. 3 shows the amount of Cr(VI) adsorbed on SAC with time under different values of solution pHs (2.0–4.0) with respect to four temperatures at a constant ionic strength of 5×10^{-2} M $NaClO_4$. It is evident that all the kinetic curves exhibit a rapid adsorption to attain the equilibrium phases. Two phases were observed in all cases: a rapid adsorption appeared within 30 min contact time, followed by a progressive and much slower uptake. In general, approximately 95% of the Cr(VI) adsorption was achieved within 1 h. After 1.5 h of contact time, the equilibrium adsorption was reached despite the variation of pH or temperature. A 2 h contact time was deemed sufficient to establish equilibrium; it was then used for the equilibrium studies. The rapid adsorption could be attributed to a surface reaction process, whereas the progressive decrease of adsorption sites results in a slower adsorption reaction [12].

In Fig. 3, the solid lines are the best fit of the PFO model to the kinetic data. Table 2 summarizes the corresponding model fitting parameters, i.e., k, the correlation coefficient (r^2), and the standard deviation (s). The high r^2 (all greater than 0.99) and the low s values (<10.5%) indicate that the experimental data were well correlated to the PFO equation. The adsorption rate constant and the amount of Cr(VI) adsorbed were found to be inversely proportional to the solution pH. In other words, an increase in the pH led to a decrease in the rate of adsorption at any temperature studied. As shown in Table 2, increasing the solution pH from 2.0 to 4.0 resulted in a decrease of k from 0.056 to 0.030 min^{-1} at 4 °C. Rate constants at temperatures other than 4 °C also exhibit a similar trend. Apparently, the rate of Cr(VI) adsorption speeds up under acidic conditions. At low pH value, specifically less than pH_{zpc}, the surface of SAC is negatively charged, enhancing the adsorption of anionic Cr(VI) by means of electrostatic attraction. As the pH increased, the attractive forces become

Table 2
Variation in the amount of Cr(VI) adsorbed on SAC and constants of PFO model fitting at different pHs and temperatures

Temperature (°C)	pH	q_e (mg/g)	k (min^{-1})	r^2	s (%)
	2.0	0.709	0.056	0.998	4.1
	2.5	0.564	0.048	0.999	3.8
4	3.0	0.436	0.042	0.995	8.9
	3.5	0.339	0.035	0.997	4.3
	4.0	0.207	0.030	0.991	10.2
	2.0	0.724	0.064	0.999	2.0
	2.5	0.577	0.059	0.999	2.4
14	3.0	0.456	0.052	0.997	5.6
	3.5	0.362	0.047	0.993	7.5
	4.0	0.219	0.041	0.998	3.2
	2.0	0.912	0.075	0.998	3.1
	2.5	0.580	0.069	0.994	6.2
24	3.0	0.460	0.062	0.991	8.2
	3.5	0.397	0.057	0.997	5.3
	4.0	0.262	0.051	0.999	2.7
	2.0	1.389	0.178	0.977	10.9
	2.5	0.591	0.149	0.994	3.8
40	3.0	0.528	0.128	0.997	2.5
	3.5	0.495	0.096	0.998	2.7
	4.0	0.270	0.070	0.994	4.9

smaller and this consequently results in decrease of adsorption.

It is also evident that the amount of Cr(VI) adsorbed and rate constant increases with increasing temperature at any pH studied. The rate constant listed in Table 2 was used to estimate the activation energy (E_a) of the adsorption process. The Arrhenius equation given as follow was used to calculate E_a:

$$\ln k = \frac{\ln(A) - E_a}{RT} \quad (5)$$

where A is the pre-exponential factor, R is the universal gas constant (1.987 cal/mol K) and T is the absolute temperature (K). From the slope of an $\ln k$ versus $1/T$ plot, the pre-exponential factor were calculated to be 1008, 692, 538, 189 and 45 for pH 2.0, 3.0, 3.5, 4.0 and 4.5, respectively. The values of 'A' suggested that the rate of adsorption would drastically increase at a higher temperature and lower pH conditions. The apparent activation energies were found to be 5.47, 5.33, 5.26, 4.74 and 4.01 kcal/mol for pH 2.0, 3.0, 3.5, 4.0 and 4.5, respectively. A diffusion controlled process has an activation energy below 6.0–7.2 kcal/mol, whereas for the chemical-controlled reaction, it has higher values [13]. The magnitude of activation energy also gives the type of adsorption, i.e., physical or chemical. Researchers [14] suggested that the value of activation energy ranges from 1.2 to 9.5 kcal/mol for a physisorption mechanism while the range of 9.5–95.5 kJ/mol for chemisorption mechanism. The activation energy obtained in this work ranged from 4.01 to 5.47 kcal/mol suggested that the adsorption was diffusion controlled and was governed by interactions of physical nature. Similar E_a values have been reported for the study of Cr(VI) adsorption [15–17].

3.2. Equilibrium studies

3.2.1. Effect of pH on the adsorption equilibrium

Solution pH is the most important variable affecting the adsorption characteristics. Fig. 4a depicts the percentage of Cr(VI) removed as a function of equilibrium pH with 1 g/L of SAC solution containing 4.12 mg/L of Cr(VI). Blank test without adsorbent in the mixed suspension was run in parallel to monitor the interference of the adsorption procedure being conducted. As seen in Fig. 4a, no removal can be found for the blank test indicating that the SAC is the sole adsorbent providing for Cr(VI) removal. Fig. 4a shows the adsorptive removal is small in the alkaline region. The marked adsorption was observed under acidic condition and the amount adsorbed decreased with increasing pH. Up to 100% of Cr(VI) removal was achieved with 4 g/L of SAC in a solution containing 4.12 mg/L Cr(VI). In general, chromate ion adsorption decreased abruptly at pH 2.0–4.0 value and then progressively decreases or remains almost constant over a wide pH range (4.0–7.0). The results shown in

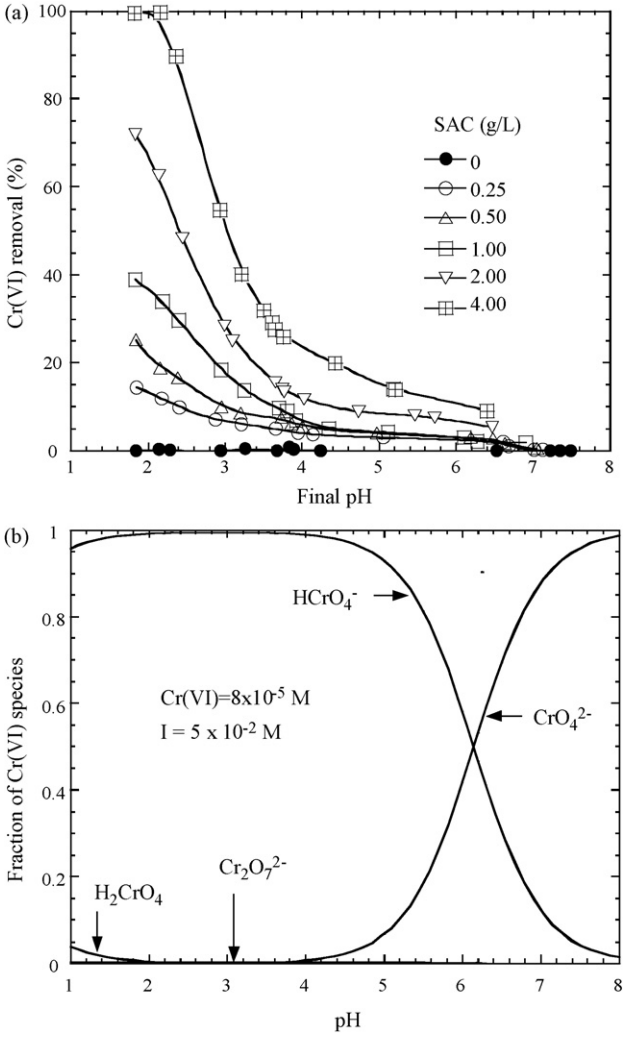

Fig. 4. (a) Adsorption efficiency of Cr(VI) as a function of pH. Conditions: initial Cr(VI) 4.12 mg/L, $NaClO_4$ 5×10^{-2} M, 24 °C. (b) Distribution diagram of Cr(VI) species as a function of pH based on the equilibrium constants listed in Table 3.

Fig. 4 demonstrate that the adsorption was closely related to the surface charge of the SAC. As mentioned previously, montmorillonite is the main component of SAC. Due to ionization of functional groups developed on the surface of the clay edges, the surface charge of this clay is pH-dependent. Therefore, when the solution pH is less than the value of pH_{zpc} (3.8), the SAC possesses a positively charged surface which would be favorable for anionic ion adsorption. The active surface functional groups at the clay edges have been well recognized as the silanol (Si–O^-) and aluminol (Al–O^-) sites as the main constituents of this clay are SiO_2 (65–75%) and Al_2O_3 (15–20%) [12]. Based on the speciation diagram shown in Fig. 4b, the major chromate ions coexisting in solution are $HCrO_4^-$ and CrO_4^{2-} for the Cr(VI) concentration of 4.12 mg/L (8×10^{-5} M). Since 99.1% of the Cr(VI) species belong to $HCrO_4^-$ at pH lower than 4, the removal of Cr(VI) can be attributed to the adsorption of $HCrO_4^-$. On the other hand, at pH > 4 (roughly around the value of pH_{zpc}), the adsorbed chromate species are expected to be $HCrO_4^-$ and CrO_4^{2-}. Despite the fact that adsorption affinity of CrO_4^{2-} is higher than OH^- and it may exchange with OH^- ion [20], the adsorbed amount is significantly low at $pH > pH_{zpc}$.

Metal adsorption onto hydrous solids such as metal oxides and clay minerals is a surface coordination process that can be modeled thermodynamically as a complex reaction between surface sites and adsorbate [19,21]. The developed surface sites for a hydrated adsorbate are formulated as following expressions:

$$S\text{–}OH_2^+ = S\text{–}OH^\circ + H^+ \quad (6)$$

$$S\text{–}OH^\circ = S\text{–}O^- + H^+ \quad (7)$$

where S represents the SAC surface sites accounted for both Si– and Al– surfaces, S–OH_2^+, S–OH and S–O^- refer to protonated, neutral and deprotonated surface hydroxyl functional groups, respectively. It is well known that pH_{zpc} is a master variable to characterize the deprotonation of the amphoteric surface functional groups. In this work, at pH value below pHzpc, the positively charged SAC surface (S–OH_2^+) would be favorable for the anionic hydrochromate, $HCrO_4^-$, adsorption whereupon the coulombic interaction forces can readily take place. Noted that the hydro-chromate, $HCrO_4^-$ (Fig. 4b), ion is now the dominant species involved in the formation of surface complexes below pH_{zpc}. Hence, the adsorption capacity of $HCrO_4^-$ will decrease due to the decrease of attractive surface charge of SAC. In Fig. 4a, one can still see that a small amount of Cr(VI) was removed between pH 3.8 and 7.0 whereupon pH is greater than pH_{zpc}. At this region, the neutral surface hydroxyl functional group, S–OH°, may be the sole active site providing for both $HCrO_4^-$ and CrO_4^{2-} adsorption.

As the solution pH increases, not only less functional group (S–OH°) is deprotonated but also more OH^- is now competing with the coexistence of $HCrO_4^-$ and CrO_4^{2-} ions (Fig. 4b) for the active surface sites. Consequently, it is difficult for them to form complexes and the adsorbed amount will decrease. Thus, the possible mechanisms for the pH-dependent Cr(VI) adsorption onto SAC are proposed as follows:

Table 3
Equilibrium constants (log K) for Cr(VI) hydrolysis reactions

Equilibria	log K (I = 0 M)[a]	log K ($I = 5 \times 10^{-2}$ M)[b]
$H_2CrO_4(aq) = HCrO_4^- + H^+$	0.20	0.382
$HCrO_4^- = CrO_4^{2-} + H^+$	−6.51	−6.145
$2HCrO_4^- = Cr_2O_7^{2-} + H_2O$	1.53	1.706

[a] Values of log K for I = 0 M from Smith and Martell [18].
[b] Activity coefficients, γ, were calculated from Davies equation [19]: $\log \gamma = -0.5 \times Z^2 \times [I^{0.5}/(1 + I^{0.5}) - 0.3I]$, where Z is the charge of ion and I is the ionic strength.

$$S\text{–}OH_2^+ + HCrO_4^- = S\text{–}HCrO_4 + H_2O; \quad \text{For pH} < pH_{zpc}\,(3.8) \quad (8a)$$

or

$$S\text{–}OH^\circ + HCrO_4^- = S\text{–}HCrO_4 + OH^-; \quad \text{For pH} < pH_{zpc} \quad (8b)$$

$$S\text{–}OH^\circ + CrO_4^{2-} = S\text{–}CrO_4^- + OH^-; \quad \text{For pH} > pH_{zpc} \quad (9)$$

where S–$HCrO_4$ and S–CrO_4^- are the formation of the bonding complexes.

3.2.2. Adsorption isotherms

The isotherms for adsorption affected by pH and temperature are illustrated in Fig. 5. The Langmuir adsorption equation was used for analyzing the batch experimental data, which is thought to be one of the most common isotherm equations for modeling a metal–surface complex system. The general form of this equation has the relationship:

$$q = \frac{K_L C_e Q_m}{1 + K_L C_e} \quad (10)$$

where q (mg/g) is the adsorption density, K_L (L/mg) is the Langmuir constant related to the affinity of the binding sites, Q_m is the saturation adsorption density (mg/g) and C_e is the equilibrium Cr(VI) concentration (mg/L). From the isotherm fitting (solid lines in Fig. 5) analysis using method of least-square based on an optimization of algorithm, the best-fitted values of Q_m, K_L and correlation coefficients, r^2, are determined and tabulated (Table 4). The high value of r^2 (>0.977) and the smoothness of all fitting curves show the applicability of the Langmuir isotherm equation. The fitting results indicate that the adsorption capacity, Q_m, and the adsorption affinity constant, K_L, are greatly affected by pH and temperature. In general, the values of Q_m and K_L increased as temperature increased and pH decreased.

3.2.3. Effects of ionic strength

Industrial wastewater normally contains a certain amount of electrolytes with a variety of ionic species. To mimic the degree of the effects of impurity on the adsorption reaction,

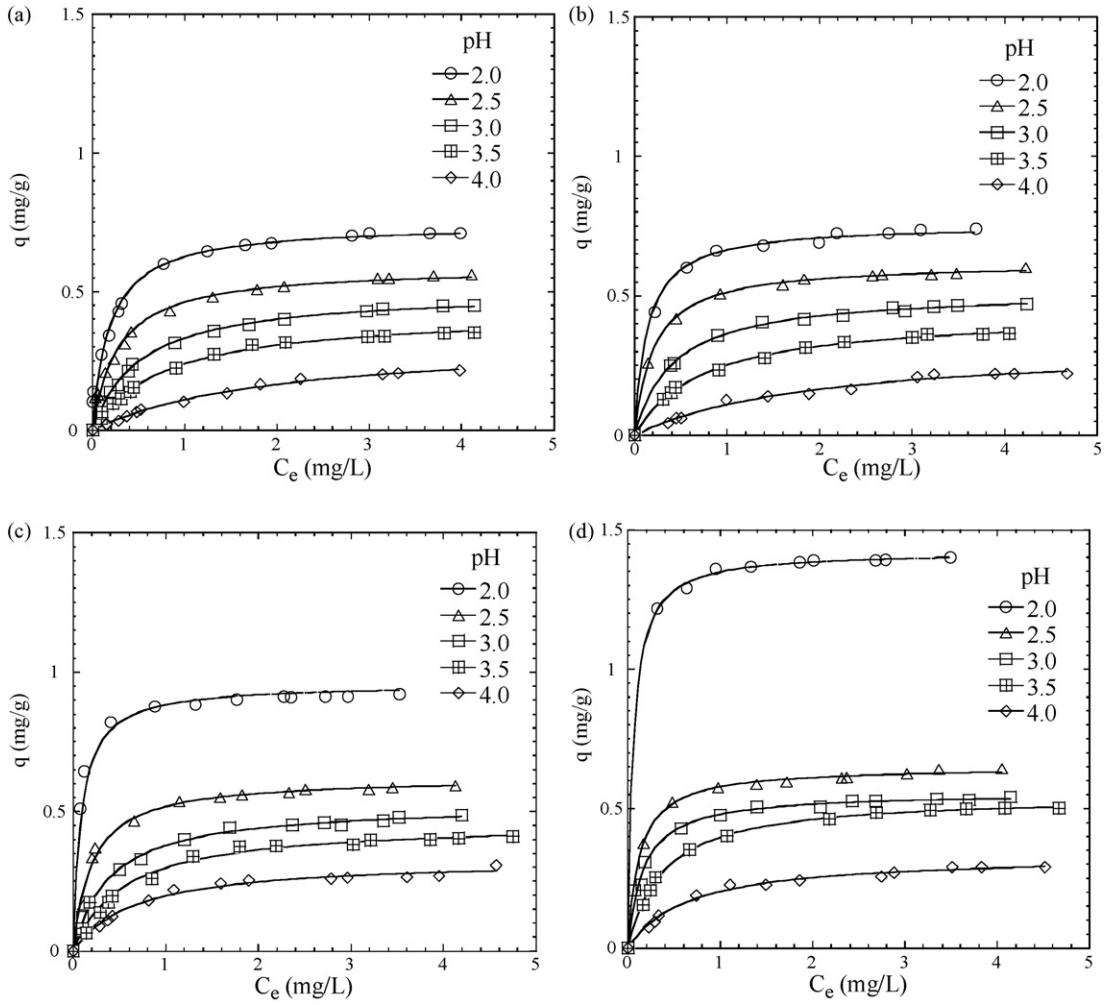

Fig. 5. Isotherms for Cr(VI) adsorption onto SAC at different pHs and temperatures. (a) 4 °C; (b) 14 °C; (c) 24 °C; (d) 40 °C. Solid lines are the best fit of Langmuir equation.

ionic strength ranging from 5×10^{-3} to 1×10^{-1} M was therefore used herein. The surface charge carried on the surface of a hydrated adsorbent relies greatly on its electrical double layer (EDL) structure. Increasing ionic strength could result in a decrease in the thickness of the EDL, thereby leading to a decrease in adsorption. The equation for calculation of the thickness of EDL (m), $1/\kappa$, associated to the ionic strength (I) is given as:

$$\frac{1}{\kappa} = \left(\frac{2F^2 I \times 1000}{\varepsilon \varepsilon_o RT} \right)^{-0.5} \tag{11}$$

where F is the Faraday constant (96,500 C/mol), ε is the dielectric constant of water (78.5) and ε_o is the vacuum permittivity (8.854×10^{-12} C/(V m)). R is the molar gas constant (8.314 J/(mol K)) and T is the absolute temperature (K). Fig. 6 shows the Cr(VI) adsorption isotherms affected by ionic strength. The solid lines showed in Fig. 7 representing the best fit of Langmuir equation to the experimental data. Table 5 lists the corresponding model fitting parameters. Results showed that an increase in ionic strength led to a decrease in the adsorption capacity and the adsorption affinity. When ionic strength was

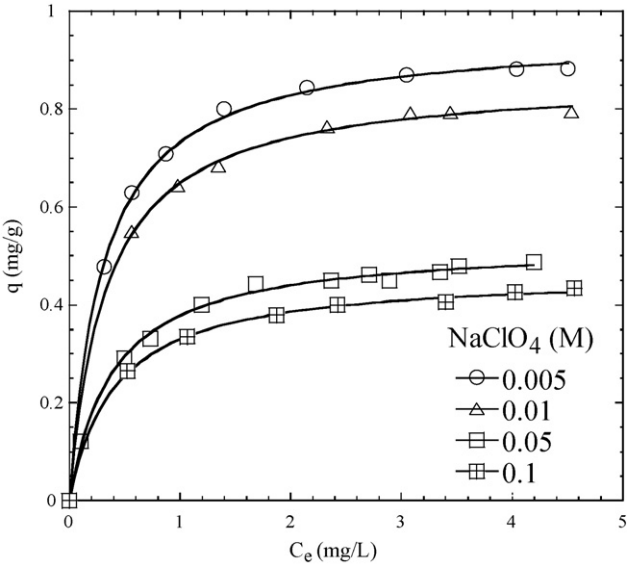

Fig. 6. Isotherms affected by ionic strengths.

Table 4
The Langmuir constants at different pHs and temperatures

Temperature (°C)	pH	Q_m (mg/g)	K_L (L/mg)	r^2
	2.0	0.743	5.339	0.981
	2.5	0.589	3.640	0.987
4	3.0	0.503	1.956	0.998
	3.5	0.427	1.274	0.997
	4.0	0.331	0.502	0.995
	2.0	0.756	7.298	0.997
	2.5	0.618	4.894	0.999
14	3.0	0.518	2.397	0.999
	3.5	0.436	1.366	0.998
	4.0	0.327	0.511	0.984
	2.0	0.957	5.037	0.983
	2.5	0.621	2.562	0.990
24	3.0	0.526	1.902	0.997
	3.5	0.462	1.829	0.977
	4.0	0.331	1.488	0.986
	2.0	1.422	18.24	0.999
	2.5	0.649	8.206	0.998
40	3.0	0.557	6.185	0.991
	3.5	0.548	2.634	0.999
	4.0	0.334	1.544	0.991

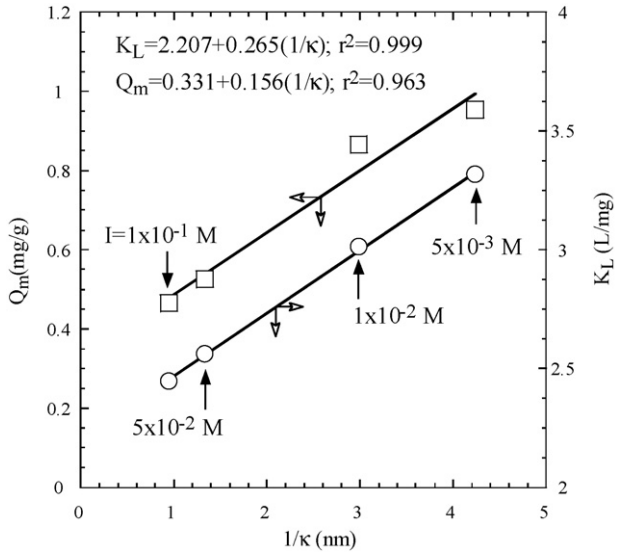

Fig. 7. Relation of $1/k$ and Langmuir constants.

increased from 5×10^{-3} to 1×10^{-1} M, Q_m decreased from 0.954 to 0.465 mg/g and the corresponding value of K_L lowered from 3.318 to 2.448 mg/g. Fig. 7 depicts the linear relationships between $1/\kappa$ and the Langmuir constants, Q_m and K_L. As indicated by Eq. (11), an increase in ionic strength would lead to a decrease in $1/\kappa$ and increase the amount of indifferent ions approaching the SAC surface. Thus, the results shown above can be attributed in part to the competition between hydrochromate ion ($HCrO_4^-$), and perchlorate (ClO_4^-) ion for surface sites as the ionic strength increased. Such adverse effect of ClO_4^- on Cr(VI) adsorption has also been reported in a study of chromium(VI) adsorption onto $ZnCl_2$ activated coir pith carbon [22].

Table 6
Thermodynamic parameters for the adsorption of Cr(VI) onto SAC

ΔG° (kcal/mol)				ΔH° (kcal/mol)	ΔS° (cal/mol K)
4 °C	14 °C	24 °C	40 °C		
−6.90	−7.33	−7.87	−8.56	6.05	47.0

3.3. Thermodynamic evaluation of the process

In order to gain insight into the possible adsorption mechanisms involved in the removal process, thermodynamic parameters for the present system including Gibbs free energy of adsorption ΔG°, changes in enthalpy of adsorption (ΔH°) and changes in entropy of adsorption (ΔS°), were calculated using the following thermodynamic functions:

$$\Delta G^\circ = -RT \times \ln(K_L) \quad (12)$$

$$\ln(K_L) = \frac{\Delta S^\circ}{R} - \frac{\Delta H^\circ}{RT} \quad (13)$$

Based on the Langmuir constants, K_L, ΔG° values are −6.90, −7.33, −7.87 and −8.56 kcal/mol, respectively, for the system of 4, 14, 24 and 40 °C. The values of ΔH° and ΔS° were determined from the slopes and intercepts, respectively, of a van' Hoff plot. Thermodynamic parameters based on the above functions are listed in Table 6. The negative value of ΔG° indicates the degree of spontaneity of the adsorption process. The higher negative value of ΔG° was found for the system with higher temperature, indicating a more energetically favorable condition for Cr(VI) adsorption. Note that the results of kinetic and equilibrium experiments showed that both the rates of adsorption and adsorption capacity indeed increased with increasing temperature. This implies that the adsorption process is spontaneous with a high preference and more efficient adsorption of Cr(VI) onto SAC at higher temperature. Generally, the value of ΔG° for an ion-exchange mechanism is in the range of −1.91 to −3.82 kcal/mol [23]. It is to be noted that ΔG° value up to 4.78 kcal/mol (20 kJ/mol) is consistent with electrostatic interaction between adsorption sites and the

Table 5
The Langmuir constants at different ionic strengths

Ionic strength (M)	Thickness of EDL $1/\kappa$ ($\times 10^{-9}$ m^{-1})	Adsorption capacity Q_m (mg/g)	Adsorption affinity K_L (L/mg)	r^2
0.005	4.238	0.954	3.318	0.999
0.01	2.984	0.865	3.013	0.999
0.05	1.334	0.526	2.562	0.997
0.1	0.943	0.465	2.448	0.999

metal ion (physical adsorption) while ΔG° values more negative than 9.56 kcal/mol (40 kJ/mol) reflect the adsorption involving charge sharing or transfer from the adsorbent surface to the metal ion to form a coordinate bond [24]. As shown in Table 6, the values of adsorption free energy, ΔG°, ranged from −6.90 to −8.56 kcal/mol, indicating that the adsorption mechanism is not attributed to ion exchange. It may be suggested that a weak surface complex reaction (Eqs. (8a) and (8b)) is the major mechanism responsible for the $HCrO_4^-$ adsorption at $pH < pH_{zpc}$. As mentioned previously, active surface hydroxyl functional groups, i.e., $Si–OH^+$ and $Al–OH^+$ attract anionic hydro-chromate adsorption. Intuitively, the adsorption process can also be enhanced by electrostatic interaction as well. It must be noted here that the magnitude of the favorable coulombic energy contribution to chromate adsorption is relatively small in comparison with the chemisorption energy [21,25]. Thermodynamically, the values of ΔG° are negative and the values of ΔH° (6.05 kcal/mol) and ΔS° (47 cal/mol K) are positive, suggesting that the adsorption reaction is spontaneous at high temperature and endothermic in nature. Endothermic adsorption of Cr(VI) onto clay was also reported by other authors [7,26].

3.4. Comparison of various low-cost adsorbents

The adsorption capacity, Q_m, and the corresponding adsorption affinity, K_L, of SAC determined from the Langmuir model were compared with those of various adsorbents for the adsorption of Cr(VI) (Table 7). All the activated carbons derived from wastes exhibited a higher adsorption capacity than that of SAC except for the activated carbon derived from coconut shells which only has a Q_m of 1.38 mg/g. The biomass based adsorbents also show a significant adsorption capacity for Cr(VI). The use of nano-sized particles has advantages of high Cr(VI) capacity (Q_m 26.04–31.55 mg/g), very short of equilibrium time, e.g., 0.08 h for modified jacobsite ($MnFe_2O_4$) nanoparticles, and low space requirements associated with adsorption-based treatment. Aside from the mentioned adsorbents, several low-cost adsorbent listed in Table 7, such as riverbed sand, coconut shell powder, wollastonite, coir pith, saw dust and rice bran exhibit significantly different Cr(VI) adsorption capacities (0.15–294 mg/g). The low adsorption capacity of SAC may be attributed in part to the small specific surface area (7.42 m^2/g) of the SAC compared to that of activated carbon. Though surface area is vital to adsorption, other parameters such as pH, temperature, organic ligands and the presence of competing cations have influence on the adsorption process to various degrees [27].

Most recently, a review article written by Mohan and Pittman Jr. [1] has compared some 200 adsorbents, including commercially available activated carbons and other low-cost alternatives, for their sorption efficiency and capacities for removal of Cr(VI) from water. The adsorption capacities of all adsorbents for Cr(VI) varied significantly; the smallest one (soya cake) was only 0.00028 mg/g and the highest one (dried anaerobic activated sludge) could go up to 577 mg/g which leads the category of low-cost adsorbents. They made an important note: comparisons of different sorbents are difficult because of inconsistencies in the data presentation. Nevertheless, it can be realized that most of the commercial adsorbents listed in Table 7 exhibit a

Table 7
Comparison of adsorption capacity, Q_m, and adsorption affinity constant, K_L, of Cr(VI) onto various adsorbents

Adsorbents	SSA (m^2/g)	pH_{zpc}	Temperature (°C)	pH	Equilibrium time (h)	Q_m (mg/g)	K_L (L/mg)	References
Riverbed sand[a]	10.24	–	25	2.5	2	0.15	0.634	[28]
Autoclaved *Aspergillus flavus*[b]	–	–	30	2.0	2.5	0.335	0.175	[29]
Wollastonite[a]	–	–	50	2.5	–	0.826	0.323	[30]
Coconut shell powder[a]	–	–	27	2.0	2	1.23	1.52	[31]
AC derived from coconut shells[c]	–	–	10	2.0	48	1.38	0.3697	[32]
Spent activated clay[a]	7.42	3.8	40	2.0	1.5	1.42	18.24	Present study
Sawdust[a]	–	–	30	3.5	2	3.6	2.36	[17]
Cactus[a]	–	–	30	2.0	–	7.082	0.00613	[33]
Activated alumina[b]	370	–	25	4.0	3	7.44	0.95	[34]
Coir pith carbon[a]	167	8	35	2.0	2	10.9	0.03	[22]
Activated charcoal[c]	1,000	5.3	40	2.0	2	12.87	2.369	[34]
TiO_2 (anatase)[c]	37.8	6.15	25	2.5	24	14.56	6.58	[25]
AC derived from coconut fibers[c]	–	–	10	2.0	48	15.99	0.022	[32]
A. philoxeroides biomass 125–250 μm[b]	–	–	25	2.0	5	20.04	0.0132	[35]
Ceria nanoparticles	–	7.4	25	3.0	–	26.81	0.706	[36]
Modified jacobsite magnetic nanoparticles	208	6.5	25	2.0	0.08	31.55	1.326	[20]
Rubber wood sawdust activated carbon[c]	–	–	50	2.0	–	65.78	0.2443	[37]
Chitin[c]	–	–	25	3.0	1	70.4	0.00967	[38]
$ZnCl_2$ activated coir pith carbon[c]	910	3.2	35	2.0	2	120.5	0.18	[22]
Chitosan[c]	–	–	25	3.0	1	153.9	0.00598	[38]
Modified chitosan beads[c]	–	6.2	25	3.0	2	256.4	0.00267	[39]
Rice bran[a]	452	–	30	2.0	1.67	294	0.243	[40]

[a] Low-cost adsorbent.
[b] Bioadsorbent.
[c] Commercial adsorbent and activated carbon (AC).

high value of surface area and provide high adsorption capacity for Cr(VI) adsorption.

Albeit the Cr(VI) adsorption capacity of SAC is much smaller than that of commercial adsorbents, the adsorption affinity constant (K_L) is the highest amongst the adsorbents stated in Table 7. The equilibrium time is not long (2 h) compared with other stated adsorbents, except for the nano-sized adsorbents. Transportation and pretreatment are the two major costs of using this low-cost adsorbent in the wastewater treatment. However, SAC which is locally available, can be obtained cheaply in a large quantity. From the environmental perspective, utilization of this industrial waste for the treatment of wastewater is a win–win strategy because it not only turns the waste into a useful product but it also saves the disposal costs.

4. Conclusions

An industrial waste, spent activated clay (SAC), was tested for its possible utilization as a low-cost adsorbent for Cr(VI) removal in wastewater treatment. Findings showed that the removal of Cr(VI) was rapid with approximately 95% of the Cr(VI) adsorption within 1 h. The adsorption kinetics data is well correlated to the pseudo-first-order equation and the rate constant increased with decreasing pH and increasing temperature. The low values of activation energy suggested that the adsorption is governed by the process of diffusion. Equilibrium studies indicated that pH played an important role in determining the adsorption characteristics. In general, the adsorption capacity decreased abruptly at pH 2.0–4.0 value and then progressively decreased or remained almost constant over a wide pH range (4.0–7.0). The fitting of a Langmuir isotherm showed that the adsorption capacities of SAC varied from 0.331 to 1.422 mg/g. Results also showed that an increase in ionic strength led to a decrease in the adsorption capacity and the adsorption affinity. It is speculated that the adverse effect of ionic strength was due in part to the competitive influence of ClO_4^- on $HCrO_4^-$ adsorption. Thermodynamic parameter ΔG° ranged from −6.90 to −8.56 kcal/mol, suggesting that weak specific chemical interaction is the major mechanism responsible for the $HCrO_4^-$ adsorption. Formation of the bonding surface complexes, S–$HCrO_4$ and S–CrO_4^- was proposed. The positive values of ΔH° and ΔS° suggested that the adsorption is a spontaneous process at high temperature and endothermic in nature. This work has demonstrated that this economically viable adsorbent, SAC, can effectively remove Cr(VI) from aqueous solutions. Since the quick removal and adsorption affinity of Cr(VI) is high, it could be an attractive Cr(VI) adsorbent for industrial wastewater treatment. Data of kinetic and equilibrium studies will be useful for future scale up of treating Cr(VI)-rich effluent, such as electroplating waste.

Acknowledgements

The work was supported by National Science Council of Republic of China (Grand No. NSC 95-2221-E-214-059). The authors express their thanks to the fellows of MANALAB, I-Shou University for supporting the SEM and EDS analysis.

References

[1] D. Mohan, C.U. Pittman Jr., Review: activated carbons and low cost adsorbents for remediation of tri- and hexavalent chromium from water, J. Hazard. Mater. B137 (2006) 762–811.
[2] U.S. Environmental Protection Agency (U.S.EPA), Edition of the Drinking Water Standards and Health Advisories, Summer, EPA 822-R-06-013, 2006.
[3] C.H. Weng, Removal of nickel(II) from dilute aqueous solution by sludge-ash, J. Environ. Eng. 128 (2002) 716–722.
[4] S. Babel, T.A. Kurniawan, Low-cost adsorbents for heavy metals uptake from contaminated water: a review, J. Hazard. Mater. B97 (2003) 219–243.
[5] A. Sari, M. Tuzen, D. Citak, M. Soylak, Adsorption characteristics of Cu(II) and Pb(II) onto expanded perlite from aqueous solution, J. Hazard. Mater. 148 (2007) 387–394.
[6] A. Sari, M. Tuzen, M. Soylak, Adsorption of Pb(II) and Cr(III) from aqueous solution on Celtek clay, J. Hazard. Mater. 144 (2007) 41–46.
[7] K.G. Bhattacharyya, S.S. Gupta, Adsorption of chromium(VI) from water by clays, Ind. Eng. Chem. Res. 45 (2006) 7232–7240.
[8] M. Akçay, Characterization and adsorption properties of tetrabutylammonium montmorillonite (TBAM) clay: thermodynamic and kinetic calculations, J. Colloid Interface Sci. 296 (2006) 16–21.
[9] American Public Health Association (APHA), Standard Methods for the Examination of Water and Wastewater, Method 503C, 21st ed., 2005.
[10] S. Lagergren, Zur theorie der sogenannten adsorption gelöster stoffe. Kungliga Svenska Vetenskapsakademiens, Handlingar, Band 24 (1898) 1–39.
[11] KaleidaGraph™ (Version 3.6), Synergy Software, Reading, PA, USA, 2003.
[12] C.H. Weng, C.Z. Tsai, S.H. Chu, Y.C. Sharma, Adsorption characteristics of copper(II) onto spent activated clay, Sep. Purif. Technol. 54 (2007) 187–197.
[13] Y.S. Ho, G.A. McKay, Comparison of chemisorption kinetic models applied to pollutant removal on various adsorbents, Trans. Inst. Chem. Eng. B 76 (1998) 332–340.
[14] B. Ozkaya, Adsorption and desorption of phenol on activated carbon and a comparison of isotherm models, J. Hazard. Mater. B123 (2005) 223–231.
[15] L. Khezami, R. Capart, Removal of chromium(VI) from aqueous solution by activated carbons: kinetic and equilibrium studies, J. Hazard. Mater. B123 (2005) 223–231.
[16] M.S. Gasser, G.H.A. Morad, H.F. Aly, Batch kinetics and thermodynamics of chromium ions removal from waste solutions using synthetic adsorbents, J. Hazard. Mater. 142 (2007) 118–129.
[17] S.S. Baral, S.N. Das, P. Rath, Hexavalent chromium removal from aqueous solution by adsorption on treated sawdust, Biochem. Eng. J. 31 (2006) 216–222.
[18] R.M. Smith, A.E. Martell, Critical Stability Constants Inorganic Complexes, vol. 4, Plenum Press, New York, 1977.
[19] R.M. Stumm, J.J. Morgan, Aquatic Chemistry, John Wiley & Sons, New York, 1995.
[20] J. Hu, I.M.C. Lo, G. Chen, Fast removal and recovery of Cr(VI) using surface-modified jacobsite ($MnFe_2O_4$) nanoparticles, Langmuir 21 (2005) 11173–11179.
[21] C.H. Weng, C.P. Huang, H.E. Allen, P.F. Sanders, Cr(VI) Adsorption onto hydrous concrete particles from groundwater, J. Environ. Eng. 127 (2001) 1124–1131.
[22] C. Namasivayam, D. Sangeetha, Removal of chromium(VI) by $ZnCl_2$ activated coir pith carbon, Toxicol. Environ. Chem. 88 (2006) 219–233.
[23] Y.S. Ho, J.F. Porter, G. Mckay, Equilibrium isotherm studies for the sorption of divalent metal ions onto peat: copper, nickel and lead single component systems, Water Air Soil Pollut. 141 (2002) 1–33.
[24] M.H.A.A. Abia Jr., A.I. Spiff, Kinetic studies on the adsorption of Cd^{2+}, Cu^{2+} and Zn^{2+} ions from aqueous solutions by cassava (Manihot sculenta Cranz) tuber bark waste, Bioresour. Technol. 97 (2006) 283–291.
[25] C.H. Weng, J.H. Wang, C.P. Huang, Adsorption of Cr(VI) onto TiO_2 from dilute aqueous solutions, Water Sci. Technol. 35 (1997) 55–62.
[26] S.A. Khan, R. Rehman, M.A. Khan, Adsorption of chromium(III), chromium(VI) and silver(I) on bentonite, Waste Manage. 15 (1995) 271–282.

[27] C.H. Weng, C.P. Huang, Adsorption characteristics of Zn(II) from dilute aqueous solution by fly ash, Colloids Surf. A-Physicochem. Eng. Aspects 247 (2004) 137–143.
[28] Y.C. Sharma, C.H. Weng, Removal of chromium(VI) from water and wastewater by using riverbed sand: kinetic and equilibrium studies, J. Hazard. Mater. 142 (2007) 449–454.
[29] K.K. Deepa, M. Sathishkumar, A.R. Binupriya, G.S. Murugesan, K. Swaminathan, S.E. Yun, Sorption of Cr(VI) from dilute solutions and wastewater by live and pretreated biomass of *Aspergillus flavus*, Chemosphere 62 (2006) 833–840.
[30] Y.C. Sharma, Effect of temperature on interfacial adsorption of Cr(VI) on wollastonite, J. Colloid Interface Sci. 233 (2001) 265–270.
[31] G.H. Pino, L.M.S. de Mesquita, M.L. Torem, G.A.S. Pinto, Biosorption of heavy metals by powder of green coconut shell, Sep. Sci. Technol. 41 (2006) 3141–3153.
[32] D. Mohan, K.P. Singh, V.K. Singh, Using low-cost activated carbons derived from agricultural waste materials and activated carbon fabric cloth, Ind. Eng. Chem. Res. 44 (2005) 1027–1042.
[33] M. Dakiky, M. Khamis, A. Manassra, M. Mer'eb, Selective adsorption of chromium(VI) in industrial wastewater using low-cost abundantly available adsorbents, Adv. Environ. Res. 6 (2002) 533–540.
[34] S. Mor, K. Ravindra, N.R. Bishnoi, Adsorption of chromium from aqueous solution by activated alumina and activated charcoal, Bioresour. Technol. 98 (2007) 954–957.
[35] X.S. Wang, Y. Qin, Removal of Ni(II), Zn(II) and Cr(VI) from aqueous solution by *Alternanthera philoxeroides* biomass, J. Hazard. Mater. B138 (2006) 582–588.
[36] Z.C. Di, J. Ding, X.J. Peng, Y.H. Li, Z.K. Luan, J. Liang, Chromium adsorption by aligned carbon nanotubes supported ceria nanoparticles, Chemosphere 62 (2006) 861–865.
[37] T. Karthikeyan, S. Rajgopal, L.R. Miranda, Chromium(VI) adsorption from aqueous solution by *Hevea brasilinesis* sawdust activated carbon, J. Hazard. Mater. B124 (2005) 192–199.
[38] A. Baran, E. Bicak, S.H. Baysal, S. Onal, Comparative studies on the adsorption of Cr(VI) ions on to various sorbents, Bioresour. Technol. 98 (2006) 661–665.
[39] N. Sankararamakrishnan, A. Dixit, L. Iyengar, R. Sanghi, Removal of hexavalent chromium using a novel cross linked xanthated chitosan, Bioresour. Technol. 97 (2006) 2377–2382.
[40] K.K. Singh, R. Rastogi, S.H. Hasan, Removal of Cr(VI) from wastewater using rice bran, J. Colloid Interface Sci. 290 (2005) 61–68.